Journal of Hydrology 528 (2015) 419–434

Contents lists available at ScienceDirect

Journal of Hydrology

journal homepage: www.elsevier.com/locate/jhydrol

Evaluating the effect of climate change on areal reduction factors using regional climate model projections

Jingwan Li [a], Ashish Sharma [a,*], Fiona Johnson [a], Jason Evans [b]

[a] School of Civil and Environmental Engineering, University of New South Wales, Sydney, New South Wales, Australia
[b] Climate Change Research Centre and ARC Centre of Excellence for Climate System Science, School of Biological, Environmental and Earth Sciences, University of New South Wales, Sydney, New South Wales, Australia

ARTICLE INFO

Article history:
Received 19 April 2015
Received in revised form 21 June 2015
Accepted 27 June 2015
Available online 2 July 2015
This manuscript was handled by Konstantine P. Georgakakos, Editor-in-Chief, with the assistance of Yu Zhang, Associate Editor

Keywords:
Areal reduction factor
GEV distribution
Regional climate simulation
Climate impacts
Extreme rainfall

SUMMARY

Areal reduction factors (ARFs) are commonly used to transform point design rainfall to represent the average design rainfall for a catchment area. While there has been considerable attention paid in the research and engineering communities to the likely changes in rainfall intensity in future climates, the issue of changes to design areal rainfall has been largely ignored. This paper investigates the impact of climate change on ARFs. A new methodology for estimating changes in ARFs is presented. This method is used to assess changes in ARFs in the greater Sydney region using a high-resolution regional climate model (RCM). ARFs under present (1990–2009) and future (2040–2059) climate conditions were derived and compared for annual exceedance probabilities (AEPs) from 50% to 5% for durations ranging from 1 h to 120 h. The analysis shows two main trends in the future changes in ARFs. For the shortest duration events (1-h) the ARFs are found to increase which implies that these events will tend to have a larger spatial structure in the future than the current climate. In contrast, storms with durations between 6 and 72 h are likely to have decreased ARFs in the future, suggesting a more restricted spatial coverage of storms under a warming climate. The extent of the decrease varies with event frequency and catchment size. The largest decreases are found for large catchments and rare events. Although the results here are based on a single RCM and need to be confirmed in future work with multiple models, the framework that is proposed will be useful for future studies considering changes in the areal extent of rainfall extremes.

1. Introduction

The design of hydraulic structures such as dams, spillways and culverts, requires information on the maximum amount of rainfall that could occur for a particular catchment area over a specific duration. Design rainfall estimates are generally derived from rainfall gauge measurements and therefore represent rainfall at a point rather than over a catchment. To transform the point design rainfall to an appropriate areal average design rainfall, areal reduction factors (ARFs) are commonly used.

The ARFs account for the fact that the extreme rainfall when averaged over the catchment area is likely to be lower than the intensity of the extreme rainfall at any individual point (i.e. gauge). This effect is more pronounced as the size of the catchment area increases, so that the ARF values are lower for larger catchments. Another factor that affects the point to areal rainfall relationship is the prevailing meteorological and climatological conditions in an area. For different types of synoptic conditions, it is possible that storm events will have different areal extents, leading to differences in the point and areal averaged rainfall relationship. The different synoptic conditions are also likely to lead to different rainfall intensities and therefore the ARFs are often found to be a function of the severity of the rainfall event. This severity is defined in terms of the frequency of occurrence, i.e., the annual exceedance probability (AEP) of the event.

There are two groups of methods used to derive ARFs. Empirical fixed-area methods (Myers and Zehr, 1980; NERC, 1975; Omolayo, 1993; Shaw et al., 2011) are computationally intensive but applicable over a comprehensive range of spatial and temporal scales. In contrast, analytical methods (Bacchi and Ranzi, 1996; Bengtsson and Niemczynowicz, 1986; Rodriguez-Iturbe and Mejía, 1974; Veneziano and Langousis, 2005) require less computation but are only applicable within limited scales as they often rely on simplified assumptions. Rodriguez-Iturbe and Mejía (1974) estimated

* Corresponding author at: School of Civil and Environmental Engineering, University of New South Wales, Sydney, New South Wales 2052, Australia.
E-mail address: a.sharma@unsw.edu.au (A. Sharma).

http://dx.doi.org/10.1016/j.jhydrol.2015.06.067
0022-1694/

ARFs using the correlation between two gauges, which was assumed to follow either an exponentially decaying distribution or a Bessel-type correlation structure. This method also assumed that the point rainfall was isotropic and Gaussian distributed with a zero mean. Bengtsson and Niemczynowicz (1986) deduced ARFs from the movement of convective storms by assuming that the rainfall intensity distribution transverse to the storm was exponential. Bacchi and Ranzi (1996) derived ARFs using a stochastic method based on the assumptions that the number of crossings of high rainfall intensity levels was Poisson distributed and that the process of crossings was stationary and independent of events. Veneziano and Langousis (2005) derived ARFs based on the assumption that rainfall intensity was multifractally scale-invariant.

Until recently in Australia, the recommended ARFs were based on the US National Weather Service method (IEAust, 1987). This method is a combination analytical–empirical method and adopted ARF values were based on data from Chicago (Myers and Zehr, 1980) and Arizona (Zehr and Myers, 1984). This method uses frequency analysis of annual maximum rainfall at pairs of stations to derive the statistical characteristics, and then estimates ARFs based on the derived statistics. Due to the concern that the precipitation characteristics in the US are not necessarily representative of the conditions in Australia, studies based on Australian local rainfall records have been conducted for most parts of Australia using the modified Bell's method, which is an empirical fixed-area approach (Jordan et al., 2013). The new Australian ARFs are considered to better capture the spatial patterns of Australian rainfall and also allow for more regional variations in the ARF relationships, although the arbitrariness of using state boundaries to define rainfall relationships could be questioned.

Generally ARFs have been calculated and used with an implicit assumption of stationarity, i.e. that the statistical properties associated with the areal patterns of extreme rainfall events will be the same in the future as in the observational record. Until recently this assumption has served as a useful basis for engineering and hydrologic design (Milly et al., 2008). But with high resolution climate simulations now available and extensive research on changes in extreme rainfall, the assumption of stationarity is now being questioned.

Both climate model and observation studies have suggested that the intensity of extreme rainfall will increase due to global warming (Alexander et al., 2006; Allan and Soden, 2008; Groisman et al., 2005; O'Gorman and Schneider, 2009; Tebaldi et al., 2006; Zhu et al., 2013). A common explanation for the increase in precipitation extremes is the Clausius–Clapeyron (C–C) relationship, which states that for a 1 K increase in temperature, the saturation pressure of atmospheric water vapor increases by about 7%, leading to more atmospheric water vapor available to produce more intense rainfall events (Radermacher and Tomassini, 2012). However, the increase of extreme rainfall does not necessarily follow the C–C scaling. Recent studies have found that temperature scaling rate for precipitation extremes can either be above or below the C–C scaling depending on various aspects including storm duration, climate region, temperature range, and the analysis method used (Hardwick Jones et al., 2010; Kanemaru and Masunaga, 2012; Lenderink and van Meijgaard, 2008; Panthou et al., 2014; Shaw et al., 2011; Westra et al., 2012).

Although there have been a number of studies into changes in the intensity and frequency of extreme rainfall affecting engineering design due to anthropogenic climate change (Jakob, 2013; Liew et al., 2013; Madsen et al., 2009; Prodanovic and Simonovic, 2007; Zhu et al., 2013), less attention has been given to possible changes in the temporal and spatial patterns of extreme rainfall. A recent study (Wasko and Sharma, 2015) using a quantile scaling approach based on data from 79 rain gauges around Australia (Wasko and Sharma, 2014) demonstrated conclusively that storm temporal patterns are intensifying with increasing temperatures. There is reason to speculate that changes may be also found in storm spatial patterns, which is an important input for flood estimation. This study presents an investigation of the likely changes in rainfall spatial patterns in the future, which is achieved by estimating ARFs derived using rainfall simulations from a regional climate model (RCM) over Sydney, Australia under present (1990–2009) and future (2040–2059) climate conditions. The advantage of using a RCM to assess climate impacts on ARFs is that the high spatial resolution of the RCM better represents the spatio-temporal patterns of precipitation and accounts for complex topographical features and land use inhomogeneity that are usually not resolved by large-scale general circulation models (GCMs).

Despite the advantage of the higher resolution, RCMs are still prone to biases and cannot simulate processes at a point scale, which is the reference scale traditionally used in deriving ARFs. This paper presents a novel approach for estimating ARFs for future climates in the absence of future point scale information. The RCM skill in simulating the area-grid relationship is evaluated for the current climate before future changes in the ARFs are considered. Following standard practice for climate model assessments (Argüeso et al., 2012), the ARFs derived from the RCM driven by the reanalysis data are first examined for the current climate. Then the GCM driven RCM is evaluated in terms of reproducing the observed area-grid relationship of extreme rainfall. Finally, the model-simulated changes of ARFs are evaluated and the statistical significance of these changes is tested.

2. Data

2.1. Observational data

The observation-based ARFs used in this study are based on the equations derived by Jordan et al. (2013) for New South Wales (NSW) and the Australian Capital Territory (ACT) for durations between 1 and 120 h, catchment areas between 1 and 10,000 km^2, and AEP between 1% and 50%. The derivation of these equations is different for long durations (18–120 h) and short durations (less than 18 h). Long duration ARFs were estimated from the rainfall record at more than 6000 stations across NSW and ACT using the modified Bell's method (Siriwardena and Weinmann, 1996). These results indicated that ARFs decrease with catchment area and AEP, but increase with storm duration. Therefore, ARFs for long duration can be expressed as a function of these three factors, with the AEP effect found to be relatively small compared with catchment area and rainfall duration. As such, the ARF equations for long duration were derived in two stages. The relationship of ARF with catchment area and rainfall duration was first established for an AEP of 50%, and then the effect of AEP is added as an adjustment term. However, for short duration ARFs, observed rainfall over this region was not used due to the sparse gauge density. Instead, the 1-h ARFs published in the UK Flood Studies Report (NERC, 1975) were assumed to be applicable to this region. These were used with station-based NSW estimates of the 18-h ARFs for an AEP of 50% to interpolate the ARFs for durations in between. Since the ARFs in the UK Flood Studies Report are independent of AEP, the ARFs for short durations are also independent of the return period. Fig. 1 shows the variation of ARFs with catchment area, rainfall duration and AEP (Jordan et al., 2013).

2.2. Model simulated data

The data used to evaluate the climate impact on ARFs are from regional climate simulations over the greater Sydney region using

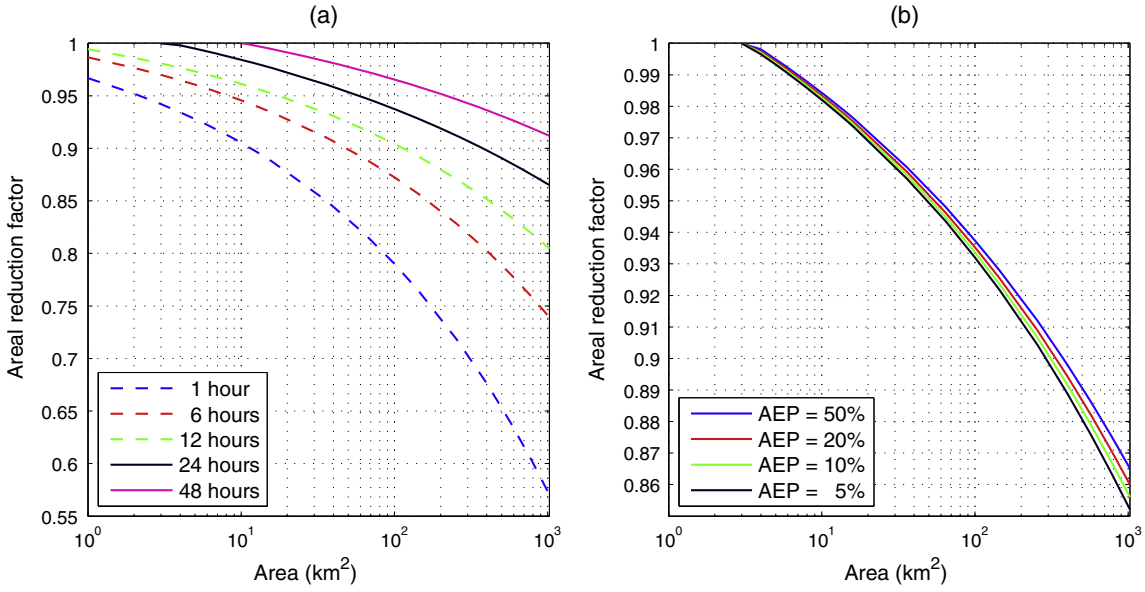

Fig. 1. ARF curves for the NSW (a) for the 50% AEP for varying rainfall durations and (b) for 24-h duration for AEP between 50% and 5% (plotted using equations in Jordan et al. (2013)).

a high-resolution Weather Research and Forecasting (WRF) model driven by CSIRO MK3.5 General Circulation Model (GCM). Fig. 2 shows the domain of this high-resolution WRF model, which extends to the Hunter Valley in the north, Jervis Bay in the south and Orange in the west. Within this WRF domain, there are 150×145 grid cells. The outermost five grids (i.e. rows or columns) along the border of the domain form the boundary relaxation zone where boundary transitional features persist, such as sharp gradients in precipitation (Räisänen et al., 2004). These five grids and the adjacent three grids, as shown by the two red rectangles in Fig. 2b, are excluded from the analyses to ensure that the results are not affected by the boundary transitions. The ocean area of the WRF domain is also excluded in this study since ARFs over ocean are not of practical use. The minimum temporal and spatial resolutions of the model output available for this study are 1 h and 2 km, respectively. The cloud microphysics scheme used by this model is the Thompson microphysics scheme (Lee et al., 2011). Details of the WRF model set up are provided in Argüeso et al. (2013a, 2012). Due to the computational demands of running such a fine resolution model 20 year simulations have been carried out for the current climate (1990–2009) and the future climate (2040–2059). Only one future emission has been modeled, which is the SRES A2 emission scenario (IPCC, 2000). The WRF simulations are driven using global boundary conditions from NCEP/NCAR Reanalysis Project (NNRP) and the CSIRO MK3.5 GCM. The 2 km resolution domain is nested within 10 km and 50 km resolution domains that have been extensively evaluated and analyzed (Evans and McCabe, 2010, 2013; Evans and Westra, 2012). This 2 km RCM has also been successfully adopted in a number of studies (Argüeso et al., 2013a, 2013b, 2015). Although this RCM considerably overestimated the light precipitation events (<10 mm day^{-1}), the extreme events are simulated reasonably well with respect to station data (Argüeso et al., 2013a).

3. Estimating ARFs using gridded rainfall

3.1. Rationale

As discussed above, ARFs measure the reduction in rainfall intensity of areal average rainfall compared to point rainfall for extreme events. For the modified Bell's method (Siriwardena and Weinmann, 1996) the frequency curves of point rainfall and areal average rainfall are calculated for each catchment. The ARFs are then calculated as the ratio of these frequency curves for a selection of events with different frequency of occurrence, which allows the ARF to vary with AEP where appropriate (Jordan et al., 2013). Alternative methods of calculating ARFs may obscure this ARF–AEP relationship due to the pooling of data across events of all sizes (Siriwardena and Weinmann, 1996). The modified Bell's method is represented by Eq. (1).

$$\mathrm{ARF}(A, \Delta t, \mathrm{AEP}) = \frac{X(A, \Delta t, \mathrm{AEP})}{X(P, \Delta t, \mathrm{AEP})} \tag{1}$$

where $X(P, \Delta t, \mathrm{AEP})$ represents the rainfall intensity at a point location (P) for duration Δt and annual exceedance probability AEP, and $X(A, \Delta t, \mathrm{AEP})$ is the areal average rainfall intensity over area A for the same AEP and duration as the point rainfall.

However, Eq. (1) cannot be used with model simulations of the future climate due to the absence of the point rainfall data. Therefore, an adjustment was made to Eq. (1) by introducing an additional term, $X(G, \Delta t, \mathrm{AEP})$, which represents the rainfall intensity over a grid cell (G). With this adjustment, Eq. (1) is split into two ratio terms as shown in Eq. (2).

$$\mathrm{ARF}(A, \Delta t, \mathrm{AEP}) = \frac{X(A, \Delta t, \mathrm{AEP})}{X(G, \Delta t, \mathrm{AEP})} \times \frac{X(G, \Delta t, \mathrm{AEP})}{X(P, \Delta t, \mathrm{AEP})} \tag{2}$$

On the right hand side of Eq. (2), the first term represents the area-grid relationship in the spatial distribution of rainfall, while the second term is simply the areal reduction factor for the area of one grid cell (i.e. 4 km^2) to a point, which is assumed to remain constant over time. This assumption will be verified by the results presented in Section 4.3. With this assumption, the potential change of the ARF in the future, which is of interest in this study, only depends on the area-grid relationship of the spatial rainfall distribution. Therefore, the change of the ARF is examined by the ratio of the area-grid relationship between a future climate projection and a current climate simulation.

It should be noted that the RCM simulations are likely to contain biases. It is possible to correct biases of the model simulation for the current climate by using observational data (Argüeso et al.,

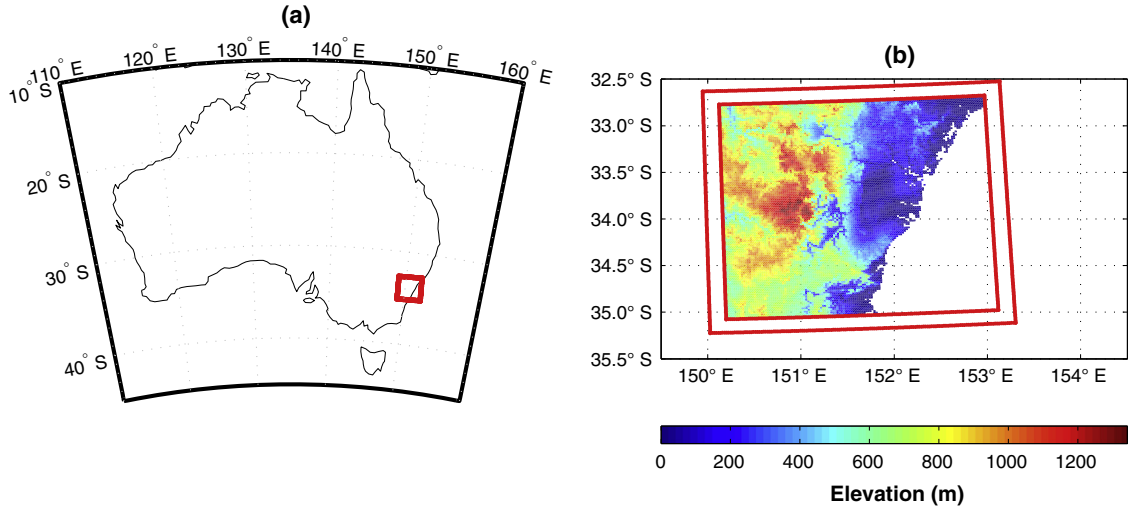

Fig. 2. WRF domain indicated by the red rectangle on the left panel zoomed in with topography on the right panel. The outmost 8 grids along the boundary indicated by the red rectangles are excluded in the analysis. (For interpretation of the references to color in this figure legend, the reader is referred to the web version of this article.)

2013a). As the aim of the current study is to assess changes in ARFs, the need for such bias correction is reduced under the assumption that the biases are multiplicative and will cancel out when the ratio of the two extreme rainfalls is calculated. For the future climate projections where observations are not available, bias correction requires the assumption that the biases are stationary (Gudmundsson et al., 2012; Maurer et al., 2013). In this study, this assumption specifically entails that the biases of extreme precipitation simulated by the RCM are stationary and multiplicative so that when the ratio of the area rainfall to grid rainfall relationship is calculated the biases will cancel out.

Due to the sparse coverage of sub-daily rainfall gauges in the study area (Johnson et al., 2012), the evaluation of RCM ARFs is carried out using the area-grid part of ARF relationship in Eq. (2), which is represented by $ARF^{ag}_{WRF/NNRP}$ or $ARF^{ag}_{WRF/MK3.5}$ depending on the boundary conditions (NNRP or CSIRO MK3.5), and comparing to the published Australian relationships (Jordan et al., 2013) at the native scale of the RCM. The original ARF estimated by Jordan et al. (2013) depicts the area-point relationship of extreme rainfall, which needs to be converted into the area-grid relationship (ARF^{ag}_{obs}) in order to compare with the RCM ARFs. The conversion function is as

$$ARF^{ag}_{obs}(A, \Delta t, AEP) = \frac{ARF_{obs}(A, \Delta t, AEP)}{ARF_{obs}(G, \Delta t, AEP)} \quad (3)$$

where $ARF_{obs}(G, \Delta t, AEP)$ is the observation-based ARF for a catchment of one RCM grid size (in this case 4 km^2) and $ARF_{obs}(A, \Delta t, AEP)$ is the observation-based ARF for the catchment area of interest that is larger than one grid size.

The conversion process is best explained through the following example. Suppose the catchment area of interest is 64 km^2 (i.e. 4 grid cells by 4 grid cells). The observed area-point ARF in the study area will be 0.89 for a 6-h storm event with a 50% AEP (see red[1] dashed curve in Fig. 1a). The area-point ARF for the same storm at the native RCM resolution (1 grid cell or 4 km^2) is 0.94. Therefore, the area-grid ARF is 0.89/0.94 or 0.95, which represents the observed reduction in rainfall intensity going from a catchment area of 4 km^2 to a catchment area of 64 km^2.

[1] For interpretation of color in Fig. 1, the reader is referred to the web version of this article.

3.2. Details of the area-grid relationship derivation

For the WRF domain, ARFs have been calculated for a range of catchment areas and rainfall event durations. For the larger catchment areas and longer durations, the rainfalls were estimated by aggregating the native WRF resolution of 4 km^2 and 1 h to larger spatial and temporal scales. The catchment areas, rainfall durations and AEPs used to derive the area-grid relationship were:

- Catchment area (in km^2): 16, 36, 64, 100, 144, 256, 400, 576, 784 and 1024.
- Rainfall duration (in h): 1, 2, 3, 6, 12, 18, 24, 36, 48, 72, 96 and 120.
- AEP: 50%, 20%, 10% and 5%.

The sample catchments for each catchment size listed above were selected from the study area without overlapping. The number of sample catchments decreases with catchment size from 3065 for 16 km^2 catchments to 48 for 1024 km^2 catchments. For each sample catchment, areal and representative grid rainfall quantiles based on regionalization are estimated by following the steps presented in Section 3.3 and 3.4. This area-grid relationship of extreme rainfall can be thought of as a factor that converts the design rainfall intensity over a catchment area of one-grid size (i.e.4 km^2) into the equivalent value over a larger catchment area.

The study region is located within one of the homogeneous regions established for estimation of ARFs (Jordan et al., 2013). The ARFs estimated for all sample catchments were pooled together and the mean was calculated to represent the ARF over this homogenous region. This is based on the procedure used to estimate the observation-based ARFs for the seven different homogenous regions across the country (Jordan et al., 2013). To test the assumption of homogeneity in the study region, spatial heterogeneity of the ARFs was investigated as part of the uncertainty analysis (i.e. catchment sampling uncertainty). The results are shown in Section 4.1.

3.3. Quantile estimation of areal rainfall

The areal rainfall quantiles, which refers to the depth of rainfall that occurs with a certain probability, are obtained from the areal rainfall frequency curve. The frequency curve is estimated by fitting a Generalized Extreme Value (GEV) distribution using

L-moments (Hosking and Wallis, 2005). The GEV has previously been shown to be appropriate for Australian rainfall data (Green et al., 2012) and has been adopted in the derivation of long duration (i.e. $\geqslant$18 h) ARF in all regions of the country (Jordan et al., 2013). The procedure for estimating the extreme quantiles of the areal rainfall involves the following steps.

1. Calculate the areal rainfall over each sample catchment by taking the average of the grid rainfall within that catchment for a given duration.
2. Find the annual maximum areal rainfall (AMAR) series.
3. Calculate the first three L-moments of the AMAR series.
4. Fit a GEV distribution to the AMAR series using L-moments.
5. Estimate the rainfall depth for each selected AEP from the GEV.

3.4. Quantile estimation of representative grid rainfall

The regionalized grid rainfall quantile was estimated using regional frequency analysis (Hosking and Wallis, 2005). This approach fits a GEV distribution using the regional weighted L-moments, which are calculated from all grids within the sample catchment. The L-moments from all grids are then averaged. The idea of regionalization is that the rainfall at all locations within a catchment comes from a common probability distribution, scaled by a site specific factor. In this case the locations are assumed to be the individual model grid cells in the catchment; in traditional regionalization studies these are gauges. Therefore the regionalized rainfall is calculated by fitting a probability distribution (the GEV in this case) and scaling this by the average scaling factor for all sites.

This approach is similar to that used by Jordan et al. (2013), where the regional weighted L-moments were estimated by first calculating L-moments for each station within the sample catchment and then weighted in proportion to the record length. In this case the only difference is the substitution of station data by the grid data and that the record length at all locations is equal as they are all model derived. The detailed steps are as follows.

1. Extract the annual maximum grid rainfall (AMGR) series from each grid within a catchment for a given duration.
2. At each grid, standardize AMGR series by dividing by its mean.
3. Compute the first three L-moments of the standardized AMGR series.
4. Within each sample catchment, estimate the regional L-moments by taking the average of the L-moments at all grids within that catchment.
5. Fit a GEV distribution to each sample catchment using the regional L-moments.
6. Estimate quantiles of the GEV distribution for selected AEPs to obtain the growth factors
7. Multiply the growth factors by the weighted mean rainfall for the catchment.

There are two main assumptions that are implicit in this regionalization approach. The first assumption is in the homogeneity of the catchment which requires that all the grid cells that lie within a particular catchment come from the same (scaled) probability distribution. Hosking and Wallis (2005) provide details of homogeneity tests which can be used to check this assumption and the most common test using the 2nd and 3rd L-moments has been implemented here.

The second assumption for the regionalization is that there is little or no correlation between the extreme rainfalls in the grid cells that form each region. If there is significant correlation between adjacent locations then this can be accounted for in the estimating the uncertainty in the regionalized estimates. More correlation reduces the effective amount of data available in the region and leads to larger uncertainties in the quantile estimates. The correlation structure of the WRF simulations has therefore been considered to assess this assumption.

4. Results

This section is divided into three parts with the first presenting an evaluation of the area-grid relationships from the WRF simulation driven by the NNRP reanalysis data representing the period 1990–2009. This provides an indication of the capabilities of this RCM in simulating the temporal and spatial characteristics of extreme rainfall. Then the modeling skill of the CSIRO MK3.5-driven WRF for the same period is assessed and compared with the NNRP-driven WRF. Finally the potential changes of ARFs in the future are estimated along with significance tests on the magnitude of the projected changes.

4.1. Evaluation of area-grid relationship from NNRP-driven WRF simulation

The area-grid relationship derived from NNRP-driven WRF is compared with the ARF relationships based on station observations (Jordan et al., 2013) for the selected durations and AEPs. Fig. 3 provides a comparison of ARFs estimated from WRF/NNRP with those derived from observations for storms with 50% AEP. ARFs estimated from WRF/NNRP (solid curves) and observations (dashed curves) are plotted for different durations in Fig. 3a, c and e, with the corresponding percentage errors shown in Fig. 3b, d and f.

In general the WRF/NNRP ARFs are in reasonable agreement with the values based on observed data, particularly for storms with duration greater than 3 h where the errors are less than 4%. The ARFs are overestimated (i.e. less reduction from point rainfall) for storms with durations between 6 h and 36 h, and underestimated for storms with durations longer than 48 h. The results presented in Fig. 3 are the mean of all ARFs calculated for each catchment area size. For the 24 h duration boxplots showing the distribution of all ARFs are provided in the supplementary material (Fig. S1) along with the observed data estimates from Jordan et al. (2013). Biases in the ARFs are relatively consistent across different catchment sizes for durations longer than 3 h which suggests the WRF/NRRP simulations are correctly representing storms across a wide range of spatial scales. Future work will examine in more detail the synoptic drivers of the different rainfall events but for now we believe that these results indicate the usefulness of the WRF simulations for considering ARF changes into the future.

For the shortest duration events (1–3 h), the results from the WRF/NNRP are not quite as good with larger errors particularly for the bigger catchment areas as shown in Fig. 3a and b. The model considerably underestimates the ARFs for catchments larger than 300 km^2. It is important to note that although the observation-based ARFs are available for all the durations, only the ARFs for longer durations are derived using Australian rainfall data. Due to the sparse density of sub-daily rainfall gauges for much of Australia, the ARFs for durations shorter than 18 h were interpolated using the values from the 18-h ARF gauge based estimate for AEP of 50% and the 1-h ARF published in the UK Flood Studies Report (NERC, 1975). In addition, the UK ARFs are AEP independent, and thus the interpolated ARFs for short durations are also independent of AEP. Basing the short duration ARFs on data from the UK where storm mechanisms are likely to be different lead to some uncertainty in these ARFs. The errors found in this study suggest that there may be problems with the applicability of the UK ARFs and/or the interpolation of the observation based values which should be investigated.

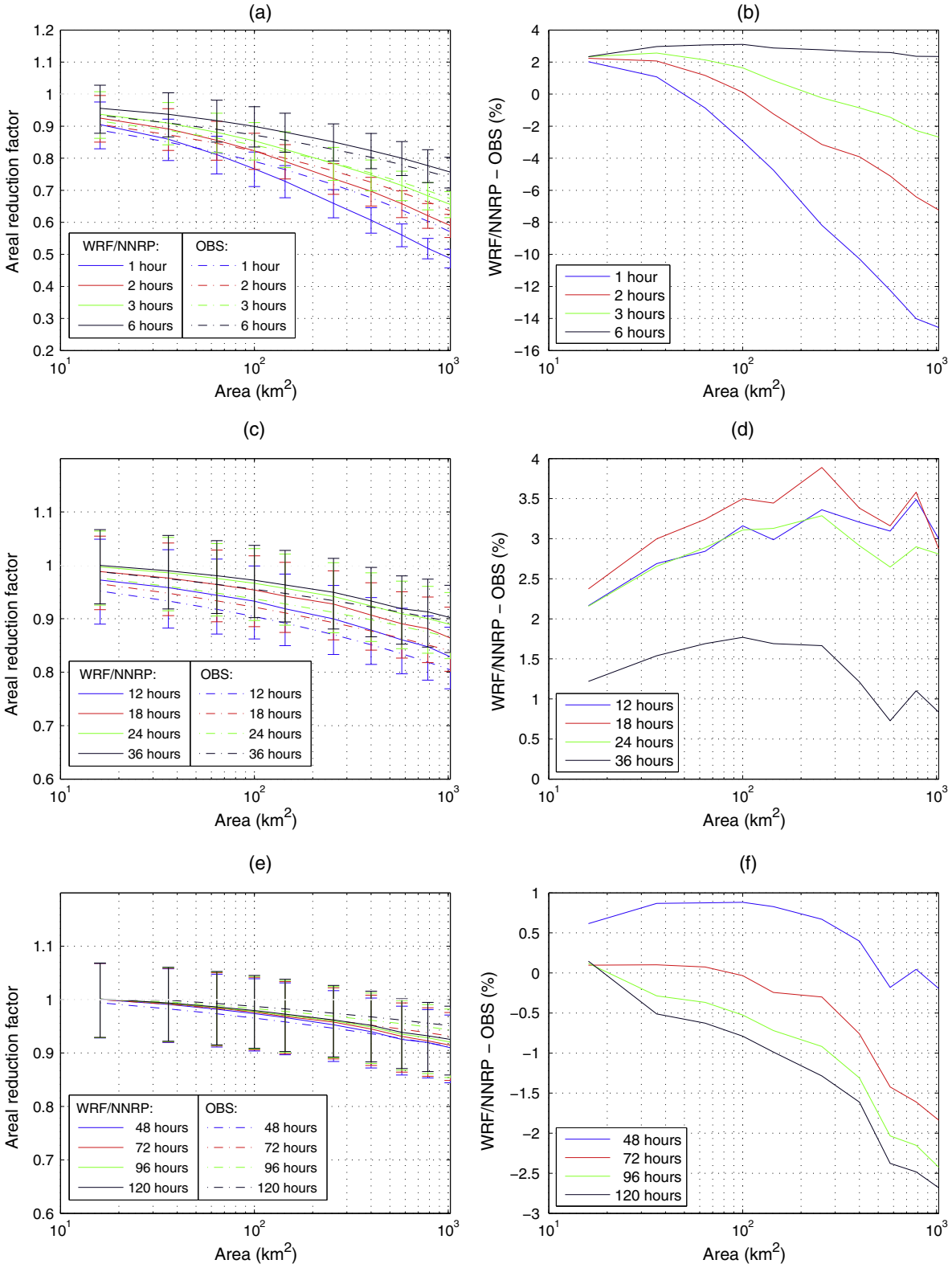

Fig. 3. ARFs estimated from WRF/NNRP simulations and from observations for storms with 50% AEP for storm duration from 1 h to 120 h. The ARFs from model simulations (solid curves) and observations (dashed curves) are plotted in (a), (c) and (e) and the percentage error is shown in (b), (d) and (f). The horizontal bars on left panels represent the interquartile range of the 500 bootstrap replicates.

As discussed previously, the areal-grid relationship varies with the severity of the storms, which is represented by the AEP. To this end, the relationship between ARFs and AEPs simulated by WRF/NNRP is compared with that seen in the observations. Since the ARFs published in UK Flood Studies Report are AEP independent, the Australian observation based ARFs for sub-daily durations also have no relationship with AEP. Therefore, the comparison of the ARF–AEP relationship between model simulations and

observations is carried out only for durations starting from 18 h. Fig. 4 shows the ARF–AEP relationship simulated by WRF/NNRP (solid curves) and from observations (dashed curves) for the storm durations of (a) 18 h, (c) 36 h and (e) 72 h, and percentage errors are shown for the same durations in Fig. 4b, d and f. It is clear that the model correctly captures the direction of the ARF–AEP relationship; rarer events have larger reductions from the point rainfall. In the model results this effect is stronger than seen in the observations. The percentage errors increase with catchment size, although in all cases the error is within ±4%.

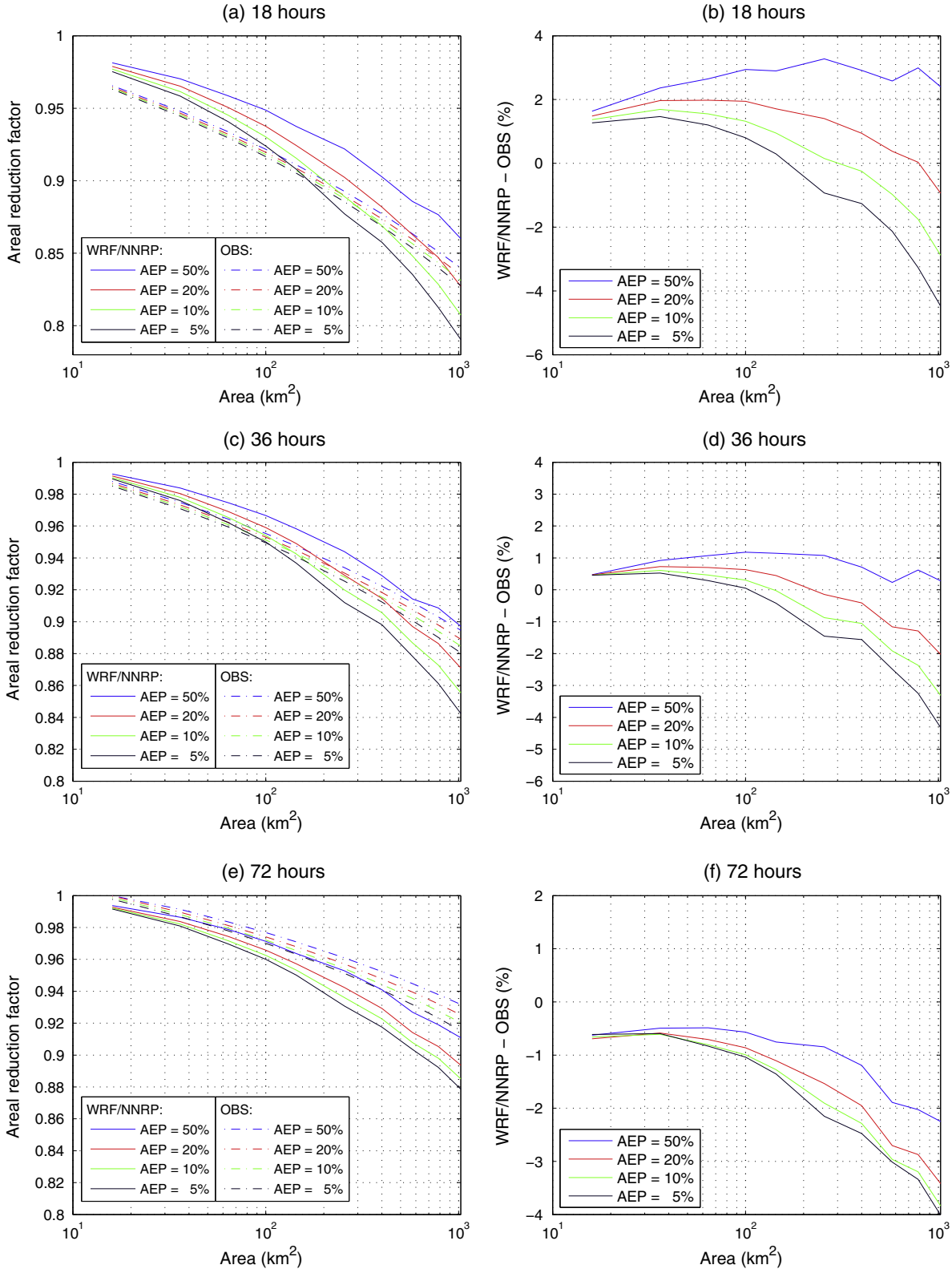

Fig. 4. ARFs estimated from WRF/NNRP simulations and from observations for storms with AEP from 50% to 5% and durations of 18 h, 36 h and 72 h. The ARFs from WRF/NNRP simulations (solid curves) and observations (dashed curves) are plotted in (a), (c) and (e) and the percentage error is shown in (b), (d) and (f).

In summary, the bias in the WRF/NNRP ARFs for daily durations and all AEPs are less than 4% with good performance across a range of catchment sizes. For sub-daily durations, the biases increase with catchment area, but it is believed that is most likely due to the use of data from the United Kingdom in deriving the observation based ARFs.

Uncertainty related to GEV fitting and catchment sampling were also evaluated. Uncertainty in GEV fitting process due to the limited data length (20 years) was assessed by the parametric bootstrap resampling method (Efron and Tibshirani, 1994), which fit 500 GEV distributions to the areal and representative grid rainfall and then estimated 500 replicates of ARFs. The uncertainty was quantified through the interquartile range (IQR) of all the replicates, which is represented by the horizontal bars in Fig. 3. It was found the relative IQR, calculated as the ratio of the interquartile range to the mean of the 500 replicates, is around 0.15 on average across different catchment sizes and rainfall durations. It is noted that the relative IQR decreases with the catchment size. This is because when the catchment size increases, more grid cells can be added into regional frequency analysis, which reduces the uncertainty related to GEV fitting. On the other hand, the relative IQR was found to increase with the rainfall duration. This is due to the fact that more grid cells are correlated as the rainfall duration increases, resulting in less amount of effective data available for regionalization. Uncertainty associated with catchment sampling, also considered as spatial variability, was examined by calculating the 5% and 95% confidence limits of the ARF values estimated from the set of all catchments of the same size. It was found that the spatial variability of ARFs estimated from WRF/NNRP simulations is comparable with the variability in the observed ARFs (Jordan et al., 2013).

4.2. Evaluation of area-grid relationship from CSIRO MK3.5-driven WRF simulation for current climate

Given the relatively small differences found in the previous section between ARFs estimated using observations, and those derived using the reanalysis-driven WRF model, it has been concluded that the WRF derived ARFs are suitable for use. The reanalysis-driven WRF is expected to provide optimal representation of the climate with minimal biases; of interest now is whether the use of a GCM for the lateral boundary conditions in WRF can lead to similar results. If this is the case, then there will be confidence in moving to the future assessment using the ARF methodology developed in this study.

The area-grid relationship estimated from CSIRO MK3.5-driven WRF under the present climate (1990–2009) is compared with observation-derived values. Results as shown in Figs. 5 and 6 are remarkably similar to those from the WRF/NNRP with little change in performance when using GCM driving data rather than reanalysis data. Fig. 5a, c and e show the ARFs estimated from WRF/MK3.5 simulations (solid curves) and observations (dashed curves) for storms of 50% AEP across a range of durations and the percentage errors are shown in Fig. 5b, d and f. Similar patterns to WRF/NNRP simulations emerge, namely:

- Relatively small errors (±4%) for durations longer than 3 h with consistent biases across all catchment areas.
- Small overestimates of the ARFs for durations from 1 to 3 h for smaller catchments.
- Errors up to −15% for larger catchment areas for durations from 1 to 3 h.

The WRF/MK3.5 model appears to perform as well as the reanalysis-driven model in simulating the areal-grid relationship.

Considering the relationship between storm severity and ARF, Fig. 6 shows that the WRF/MK3.5 simulates the same ARF–AEP relationship as shown in observations, such that the ARFs decrease with increasing storm severity. The ARF–AEP relationship simulated by WRF/MK3.5 is much closer to observations than that simulated by based on the reanalysis runs. It is also clear from Fig. 6b, c and f that the errors are more consistent across different AEPs than those estimated from WRF/NNRP. Given that the errors for the 50% AEP event are similar between the WRF/Mk3.5 and WRF/NNRP, the better results for the rarer events seen in Fig. 6 compared to Fig. 4 indicate that it is simulation of the largest events (which likely affect the GEV scale and shape parameters) particularly over larger catchment areas that leads to the smaller errors in the WRF/Mk3.5 ARFs.

4.3. Evaluation of climate impacts on ARFs

Having established that the current climate ARFs from WRF simulations are reasonably consistent with those based on the observational record, the question now investigated is how much the ARFs are likely to change in the future. The implications of using a single model for future projections are discussed in Section 5.

Fig. 7 shows the current (1990–2009) and future (2040–2059) ARFs for AEP of 50% for different storm durations in Fig. 7a, c and e with the changes shown in Fig. 7b, d and f. For these relatively frequent events, the ARFs are found to decrease when the storm duration is longer than 6 h. This result is consistent across all catchment areas. The implication is that the storm events leading to these extreme rainfalls will cover a smaller area in the future than presently and therefore the reduction from the point rainfall to catchment area rainfall should be larger. As the catchment area increases this effect becomes even more pronounced. The maximum decrease in ARFs is found for the 18 h storm and 1024 km^2 catchment size with a reduction of approximately 2%.

For the multi-day durations (bottom row of Fig. 7) the changes are generally much smaller than those found for the 6–18 h durations. Even in the current climate, ARFs for multiple day rainfall events are close to one because multiple-day rainfall totals tend to be caused by large scale weather systems such as East Coast Lows (Speer et al., 2009). These ARFs results suggest that there may not be large changes in the spatial coverage of such events in the future. This does not preclude changes to rainfall totals or the frequency of events, both of which are the subject of current research.

The most interesting results are found for the 1-h storm where increases are found in the ARFs, particularly for the smaller catchment areas, up to an area of around 250 km^2. Increases in the ARFs mean that there will be smaller reductions in point rainfall in the future. From these WRF simulations it is concluded that storm sizes in the future will be larger for the shortest duration events. The largest increases for durations from 1 h to 6 h are seen for catchments with areas around 100–300 km^2, with jumps in the ARF ratios clear in Fig. 7b and d for each of the durations. These jumps are caused by the different rate of decrease ARFs with catchment areas for current and future climates. As depicted in Fig. 7a, moving from 100 to 300 km^2 the ARFs for the current climate (solid curves) decrease faster than those for the future climate (dashed curves), leading to an increased future to current ratio of ARFs.

The issue of the statistical significance of the changes found in this study, particularly with respect to some of the small magnitude of the changes has been assessed with a non-parametric significance test. The Wilcoxon–Mann–Whiney or rank-sum test, was applied to the two samples of ARFs for the future and present climates for a given area, duration and AEP. The Wilcoxon–Mann–Whitney test was selected because it does

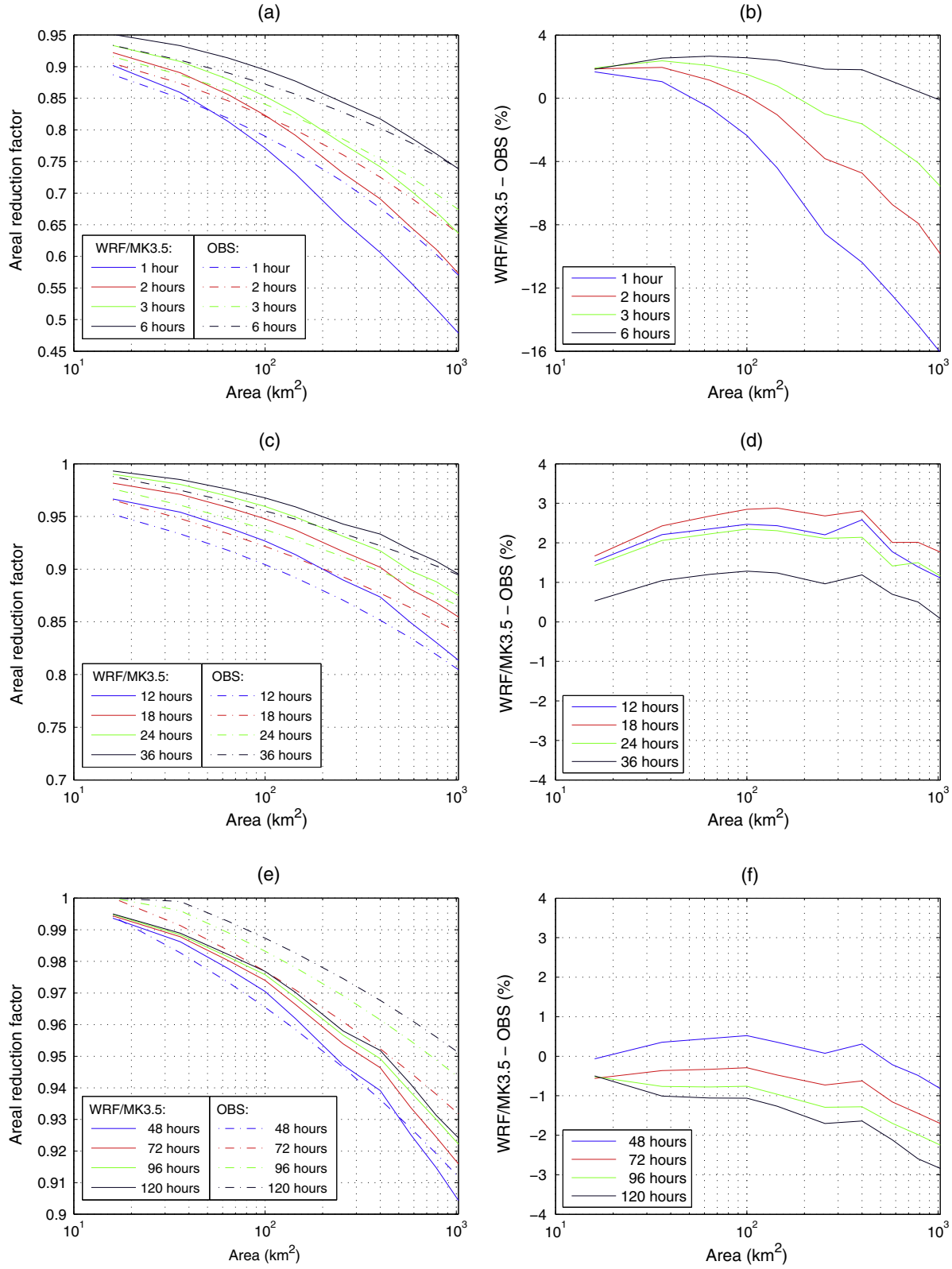

Fig. 5. ARFs estimated from WRF/MK3.5 simulations and from observations for storms with 50% AEP for different storm durations. The ARFs from WRF/MK3.5 simulations (solid curves) and observations (dashed curves) are plotted in (a), (c) and (e) and the percentage error is shown in (b), (d) and (f).

not rely on any assumption of the distribution of the ARFs to be tested. Test results are incorporated in Fig. 7 as the filled circles, which indicate where significant difference at 5% level were found between ARFs for the current and future climates. It was found (Table 1) that only 16 out of 120 combinations of areas and durations have significant changes in ARFs for the future climate for a 50% AEP. In addition, these significant changes were only found for areas smaller than 300 km^2.

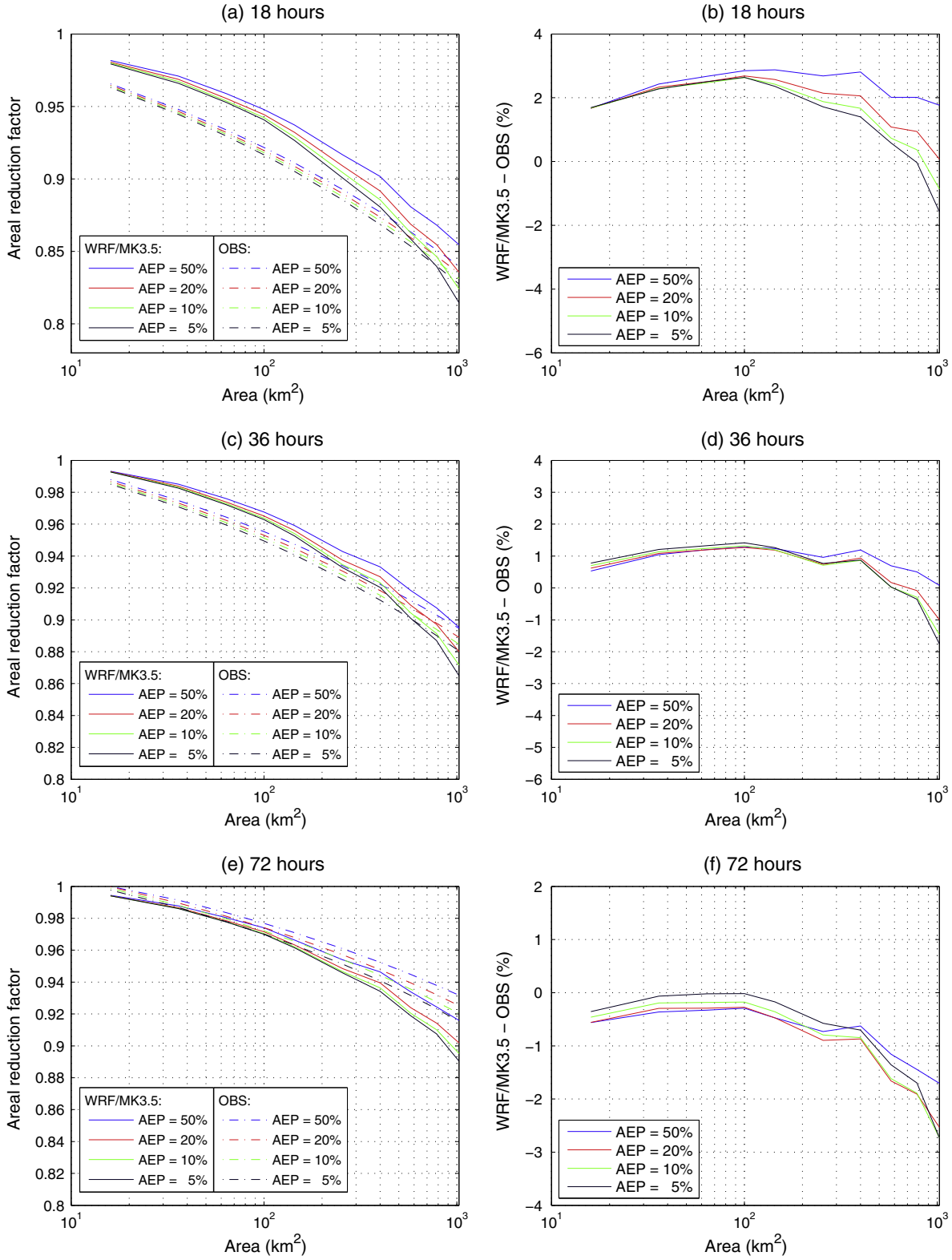

Fig. 6. ARFs estimated from WRF/MK3.5 simulations and from observations for storms with AEP from 50% to 5% and durations of 18 h, 36 h and 72 h. The ARFs from WRF/MK3.5 simulation (solid curves) and observations (dashed curves) are plotted in (a), (c) and (e) and the percentage error is shown in (b), (d) and (f).

It is also noted from Fig. 7b, d and f that the ratio of the future to current ARFs for an area of 16 km^2 is almost one (i.e. no change). This suggests that the assumption made in Section 3.1 that there will be no changes in the ARF for an area of 4 km^2 (single WRF grid cell) is appropriate. Therefore the innovative method of splitting of the ARF equation into the point-grid and grid-area components (i.e. Eq. (2)) is a useful approach for assessing future changes in the spatial patterns of extreme rainfall events.

As the ARF varies with severity of the event, it is expected that the future changes in the ARF could also vary with AEP. Fig. 8

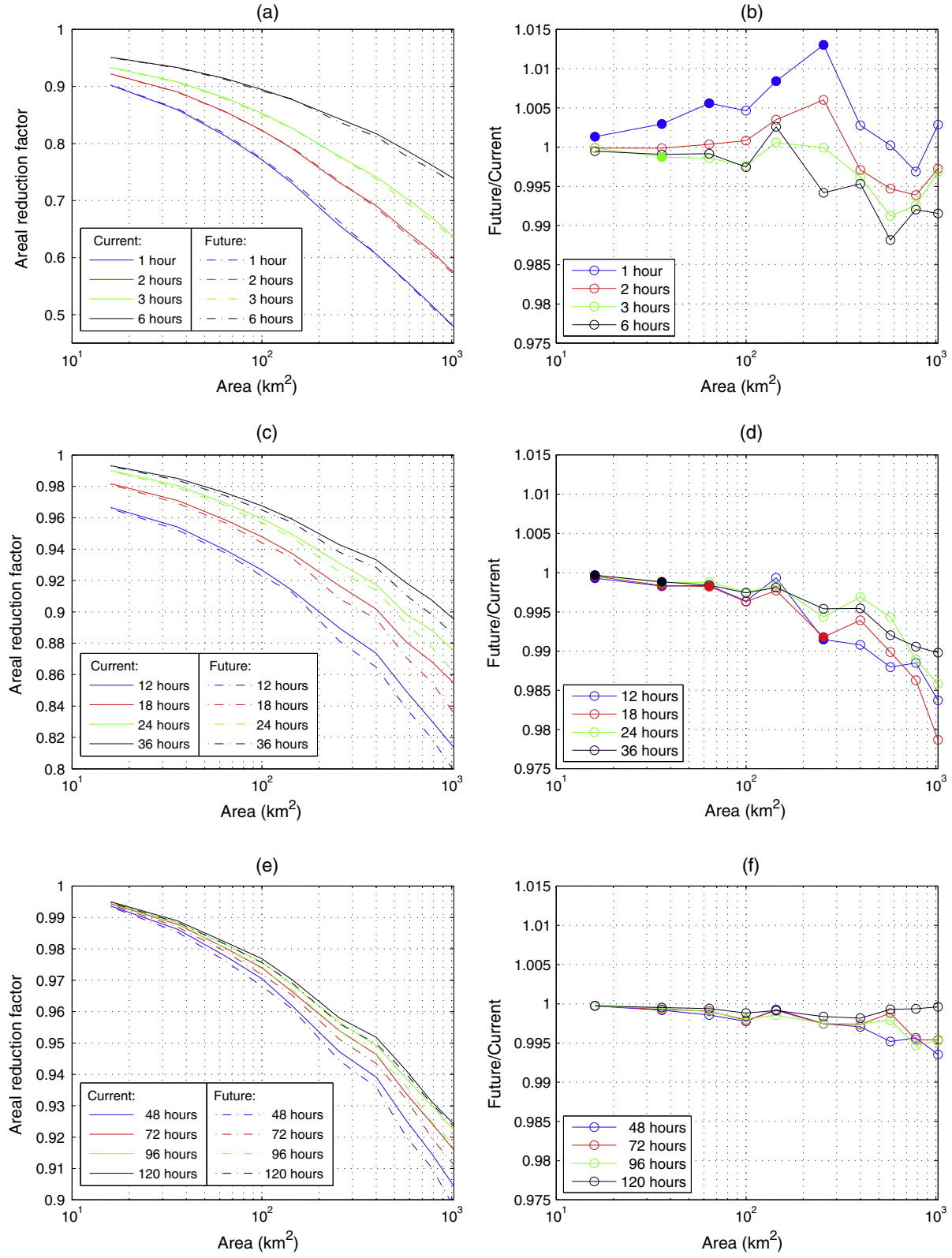

Fig. 7. ARFs estimated from WRF/MK3.5 simulations for the current climate (1990–2009, solid curves) and future climate (2040–2059, dashed curves) for storms with AEP of 50% for different storm durations are shown in (a), (c) and (e). The ratio of ARFs for the future climate to the current climate is shown in (b), (d) and (f). The filled circle indicates where the change of ARFs is significant at 5% level detected by Wilcoxon–Mann–Whitney test.

depicts the ARFs estimated from WRF/MK3.5 simulations for both current and future climates for AEPs from 50% to 5% for storm duration of (a) 1 h, (c) 24 h and (e) 72 h. As for the current climate simulations, the ARF values vary with AEP in the future and it is evident from Fig. 8d and f that this effect is even stronger in the future for daily durations. It is also noted that the magnitude of the change of ARFs tends to increase with catchment size for 24-h and 72-h storms for all AEPs examined as shown in

Table 1
The Wilcoxon–Mann–Whitney test result at a 5% significance level for different AEPs.

AEP (%)	Fraction of area-duration combinations with significant change in ARFs
50	16/120
20	40/120
10	53/120
5	66/120

Fig. 8c and e. Similar results are found for all durations longer than 6 h. We therefore conclude that the spatial coverage of the rarer events will decrease in the future even more than the 50% AEP results shown in Fig. 7. As AEP decreases, the number of combinations of areas and durations with significant changes increases, and this is mainly due to an increase in the maximum catchment area found with significant changes. For example for the largest event considered (AEP 5%), 66 out of 120 combinations of areas and durations were found to have significant change in ARFs as shown in Table 1.

For 1-h storms, the ARF changes with AEP (Fig. 8a and b) are less clear than for longer durations. For 1-h storms, the variation of the change of ARFs with respect to AEPs is not consistent across different catchment sizes as shown in Fig. 8b. However, it is clear that ARFs of 1-h storms are found to increase in the future for all AEPs, confirming the results seen in Fig. 7 for the 50% AEP event. For the longer hourly durations (2 h and 6 h) there are few changes in ARFs, thereby showing a consistent transition from the increases at 1 h to decreases at 6 h and longer events.

The spatial variability of the predicted change in the ARFs has been calculated as the coefficient of variation (CV) of the set of ARF ratios for the future climate to the present climate for each catchment area-duration combination. All combinations are shown in Fig. 9 for a range of AEP events. For the 50% AEP event (Fig. 9a), the CV value in all cases is less than approximately 0.08 (i.e. 8%). As the events become larger (decreasing AEP) the spatial variability increases, with CV values of up to 0.1 in some cases. For all AEP events, it can be seen that the CV values are lower in the top left corner of each panel and increase for increasing area and/or decreasing duration. It is therefore concluded that the most spatially consistent results across the study domain are those for smaller catchment areas and longer durations. Referring back to Fig. 8, these are the cases where very little change in the ARFs was found. It is also worth noting that the sample sizes for the larger catchment areas is much smaller than when considering areas of 16 km^2. This could be addressed in future work by comparing the results here to those for the larger NARCLIM domain of south-east Australia.

5. Discussions

While this study treated the greater Sydney region as a whole, the impacts of differences in topography and rainfall mechanisms was investigated by dividing the study domain into two separate regions, inland and coastal. The definition of inland/coastal used the delineation of Evans et al. (2012) who divided the same WRF domain based on the characteristics of the precipitation (Argüeso et al., 2011). In the present study, the area of the domain east of the Great Dividing Range was considered as one coastal region, with the remainder of the land area was classified as the inland region. The ARF changes were estimated for these two regions separately. The results showed no significant differences from those obtained by treating the entire region as a whole, and hence are not presented here.

As discussed in Section 3.4, there are two assumptions implicit in the regionalization which need to be tested. The first is whether the regions are homogenous. The regional homogeneity of the study domain was tested through the heterogeneity index (H index) (Hosking and Wallis, 2005). This index compares the between-grid variations in sample L-moments for the group of grids with what would be expected for a homogenous region, which is the sample catchment in this case. A region is considered "acceptably homogeneous" if $H < 1$, "possible heterogeneous" if $1 \leqslant H \leqslant 2$, and "definitely heterogeneous" if $H \geqslant 2$. The H index was estimated for each sample catchment for all the combinations of the selected catchment sizes and rainfall durations. It was found that on average 96% of sample catchments have H index less than 1, indicating an acceptably homogeneous region used in regional frequency analysis.

The second regionalization assumption is that the grid cells included in each region (i.e. sample catchment) are uncorrelated. The spatial correlation of annual maximum rainfall simulated by the WRF/NNRP was examined by computing the correlation coefficient and distance for all possible pairs of grids within the study region. It was found that the correlation distance was approximately 5 km for 1 h events, increasing to 25 km for 24 h events. It is thus considered that correlations in the regionalization are unlikely to be a problem for catchment areas greater than 16 km^2 for short durations and may have some limited impact on the uncertainty of the ARF estimates for longer durations. Given the large number of catchments it is believed that the mean ARF is unlikely to be biased, even though the regionalized rainfall quantiles have not accounted for the correlation in adjacent grid cells.

In evaluating model performance in terms of simulating ARFs, the observation-based ARFs were used for comparison. The discrepancies between observation-based ARFs and model derived ARFs are within 4% for storms of long durations ($\geqslant$18 h), indicating that the high-resolution RCM used in this study is suitable for estimating the potential change of ARFs. As for the ARFs for storms of short durations (<18 h), the observation-based ARFs were not derived from Australian local rainfall gauge data. Instead, the short duration ARFs were interpolated between 1-h ARFs obtained from the UK Flood Studies Report and 18-h ARFs. Therefore, it is not surprising that large discrepancies are seen between Jordan's version of ARFs and model derived ARFs. Uncertainties exist in both observation-based ARFs and model derived ARFs. Uncertainty associated with catchment sampling appears to be quite similar between the observations and model simulations. Uncertainty in GEV fitting can only be evaluated for model simulations and the results from this were presented in Fig. 3 and discussed in Section 4.1.

In quantifying uncertainty in GEV fitting, the 5% and 95% confidence limits were calculated from the 500 bootstrap replicates. It is noted that the 95% confidence limit of the ARFs plotted in Fig. 3 is not restrained to 1. During the iterations of the bootstrap resampling process, there are some occasions when the quantile of the areal averaged rainfall exceeds the quantile of the point rainfall due to the imperfectness of GEV fitting. This will lead to an ARF value exceeding 1. In existing ARFs estimates (Jordan et al., 2013), the maximum of 1 was adopted in the case of ARF exceeding 1. However, when bootstrap resampling method is used to investigate the parameter uncertainty in the GEV distribution, the genuine ARF estimates are used to construct the middle 90% confidence interval of the ARF estimates. Although the 95% confidence limit can exceed 1 here, the mean of the 500 replicates always lies below 1 and closer to the ARFs estimated from observations than if a ceiling of 1 was set for ARFs.

Uncertainty in the predicted change of ARFs related to catchment sampling was assessed through the CVs of the ARF ratios of WRF simulations of the future climate to the current climate. This type of uncertainty tends to increase with the catchment size and the return period, which is expected due to the reduced

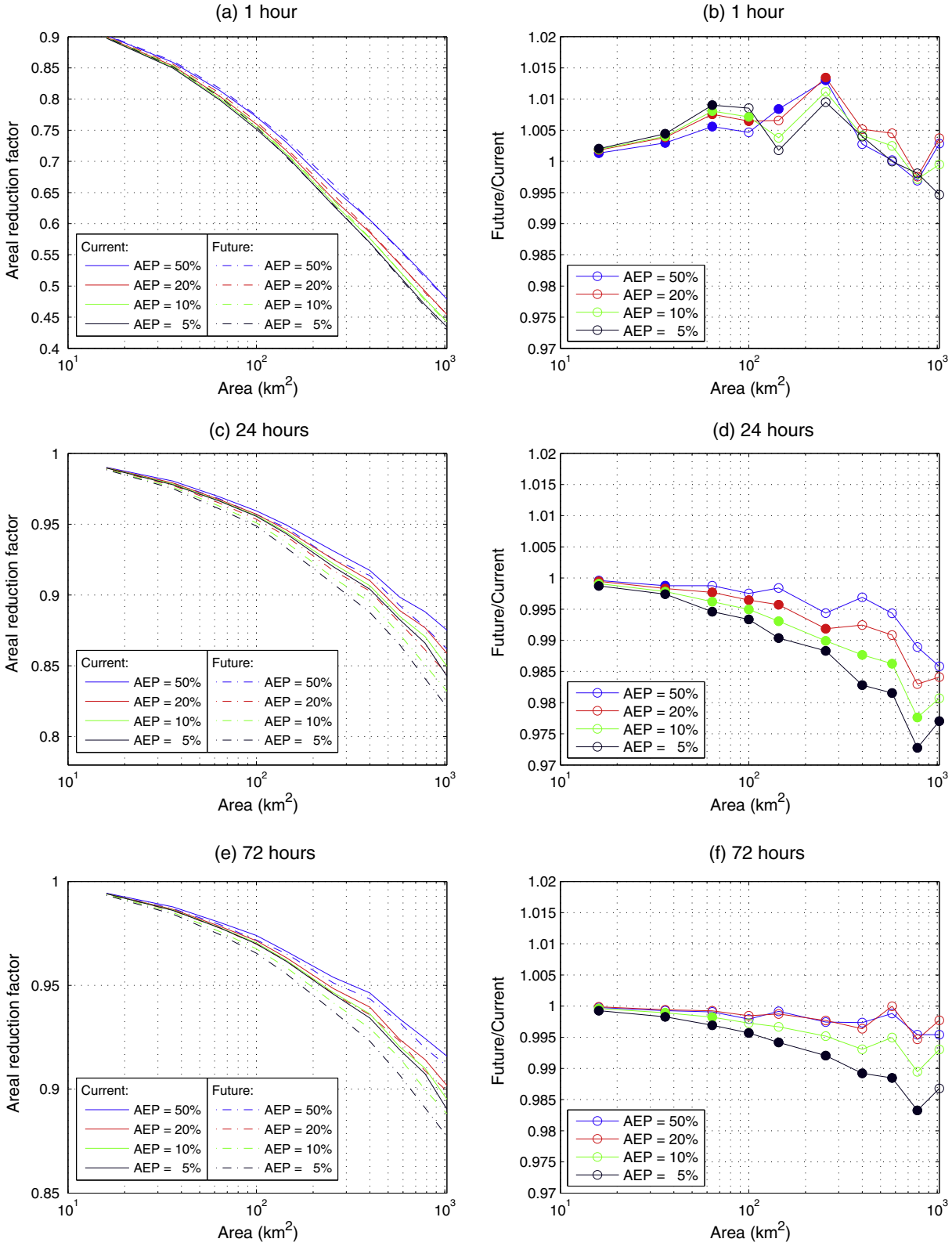

Fig. 8. ARFs estimated from WRF/MK3.5 simulations for the current climate (1990–2009, solid curves) and future climate (2040–2059, dashed curves) for storms with AEP from 50% to 5% for storm duration of (a) 1 h, (c) 24 h and (e) 72 h. The ratio of ARFs for the future climate to the current climate is shown in (b) 1 h, (d) 24 h and (f) 72 h. The filled circle indicates where the change of ARFs is significant at 5% level detected by Wilcoxon–Mann–Whitney test.

sample size and limited data length (i.e. 20 years data). However, the reason why uncertainty decreases with the rainfall duration requires future investigation.

While this is one of the first studies to comprehensively assess changes in ARFs for the future, there are a number of caveats on the results that need to be considered. The first and most obvious limitation is the use of a single GCM and an emission scenario (CSIRO MK3.5 and SRES A2). There is significant evidence in the literature that points to the uncertainty in precipitation simulations for future climates across GCMs (see the Variable Convergence Score

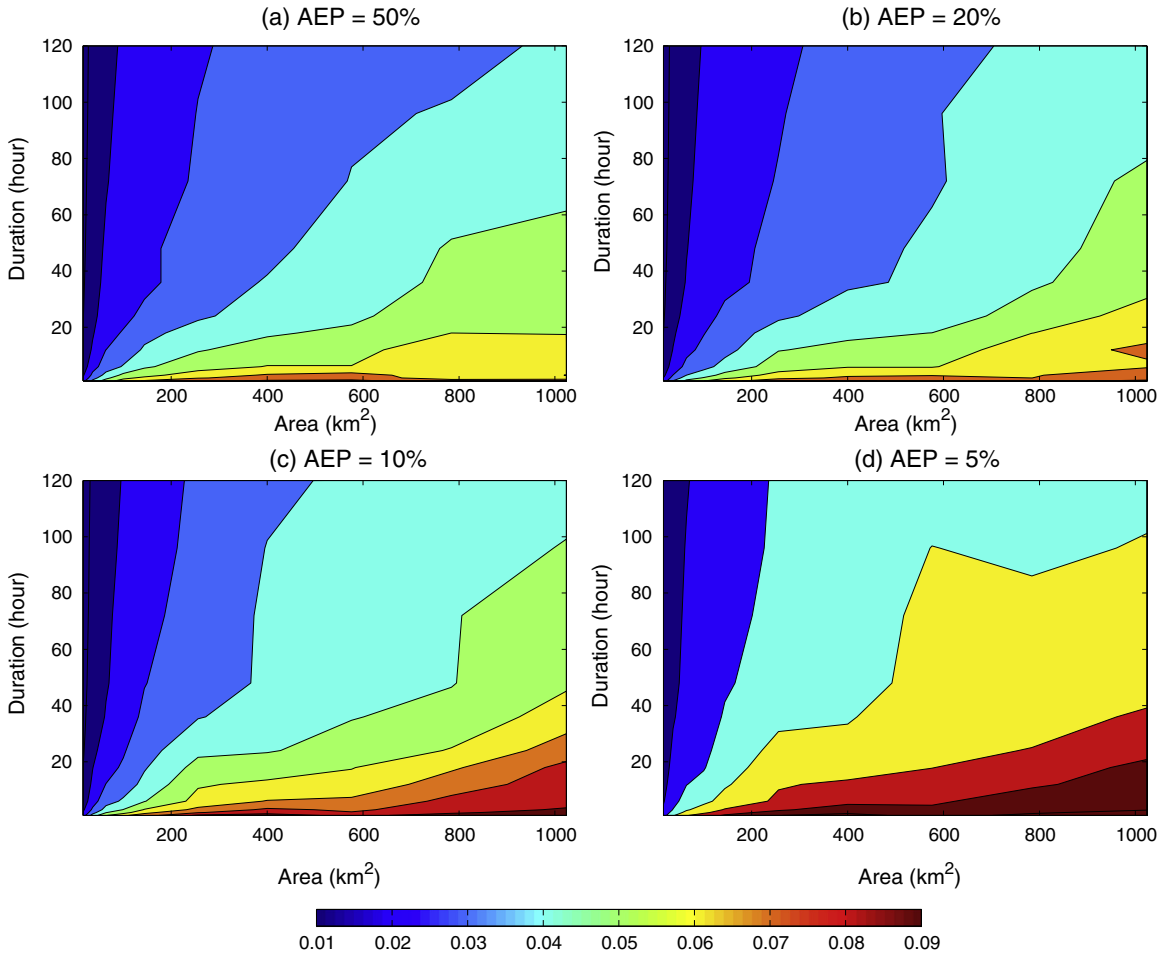

Fig. 9. The coefficients of variation (CVs) of the ratios of ARFs derived from WRF/CSIRO MK3.5 for the future climate (2040–2059) to the present climate (1990–2009) for (a) AEP = 50%, (b) AEP = 20%, (c) AEP = 10% and (d) AEP = 5% .

for precipitation for instance, reported in Johnson and Sharma (2009)). Many studies also point to the relative magnitude of structural error in GCM rainfall simulations, in comparison to other uncertainties that relate to the choice of the emission scenarios or the initialization used (Woldemeskel et al., 2012). The main difference from previous work is that in this study the focus is on ARFs rather than precipitation directly. It is thought that the ARFs should be impacted less by the presence of such errors especially if they are of a multiplicative nature (and will cancel out). In reality, while one would expect a more complex model for the GCM rainfall bias, if the over- or under-simulation of precipitation extremes is consistent across the scale of one grid cell to a larger area, the effect of this bias will be reduced when the ARF is estimated.

The second major limitation here is the use of a single regional climate model with a specified physics parameterization. It is well known that uncertainty exists in especially rainfall simulations from RCMs depending on the type of parameterization that is used. As the RCM parameterization can have a significant effect on the spatial coherence of the resulting rainfall field, this is an uncertainty that needs further assessment using alternate parameterizations. The fact that a high-resolution (2-km resolution) RCM run has been used in deriving the results reported here makes this assessment difficult, although work is underway at assessing its implications using coarser RCM runs using alternate parameterizations.

The third major limitation here is the assumption that the bias in the areal extreme rainfall is largely due to the model structure and is multiplicative. This assumption helps in deriving the ARFs for a future climate, as any biases that may be present in the areal extreme rainfall can be assumed to cancel out. This assumption is often used in climate change studies based on perturbation methods (also called delta methods) (Hay et al., 2000; Madsen et al., 1997; Wong et al., 2014). While one may question whether this assumption is valid or not, it is consistent with the many bias correction strategies adopted for hydrological applications, as discussed in Johnson and Sharma (2011). However, the implications of this and the above two assumptions on the conclusions drawn here are significant, and need to be evaluated further through additional research. Many of the issues listed above will be addressed over time as additional simulations using other GCMs and regional climates over the study area become available. Work is currently underway in this regard, and will be presented in the future.

6. Conclusions

This paper presents a new methodology for deriving ARFs using model simulations for future climate with the greater Sydney region as a case study. The advantage of the new method is that the future ARFs can be calculated without the need for point data. ARFs were derived from regional climate simulations using a high-resolution WRF model. This model was evaluated in terms of its capability of representing the area-grid relationship of extreme rainfall by comparing the ARFs derived from both reanalysis and GCM driven WRF runs to observation-based ARFs. Overall ARFs were simulated well by both WRF/NNRP and WRF/CSIRO

MK3.5 over the study area with less than 4% error for durations longer than 3 h.

For future climates, it was found that the ARFs tend to decrease for durations between 6 h and 72 h for all AEPs from 50% to 5%. However, the decrease in ARFs was not statically significant for 6-h storms with catchments larger than 100 km^2. For storm durations between 12 h and 24 h, almost all catchment sizes examined were seen significant decrease in ARFs for storms with AEP of 20% or less, indicating that in the future these storms are likely to be more localized than is the case presently. As the storm duration increases from 24 to 72 h, the cases with large AEP and area start to lose significance first mainly due to the decreasing sample size for large catchments. This finding suggests that with a larger sample size these ARF changes would likely remain significant for large AEP and area. For 72-h duration, storms with AEP less than 20% show no decrease in ARFs is significant. While the ARFs were found decrease for 6- to 72-h storms, they are expected to increase for 1-h storms for all AEPs examined and areas less than 500 km^2, which suggests that 1-h storms will be more widely distributed in the future than is the case presently. Significance tests show that the percentage of the area-duration combinations with significant change in ARFs ranges from 13% to 55% depending on the AEP. More cases were detected with significant changes in ARF for smaller AEP.

In general, changes to ARFs in the future have been neglected by the engineering and hydrologic communities. Ignorance of changes in ARFs in particular may lead to incorrect assessment of flood hazard. This study presented a framework in which changes to ARFs using future climate simulations can be assessed. For the study region considered, if our results are found to be consistent with future work using multi-model simulations, then ignoring increases in ARFs especially for shorter durations will lead to under-designed infrastructure and underestimated flood risks. Conversely areal flood risk in the future for longer duration events will be smaller than present, although increases in rainfall intensity may well offset these changes.

Acknowledgments

Regional climate data have been provided by the New South Wales and Australian Capital Territory Regional Climate Model (NARCliM) project funded by NSW Governmental Office of Environment and Heritage, University of New South Wales Climate Change Research Centre (CCRC), ACT Government Environment and Sustainable Development Directorate and other project partners. This work was made possible by funding from the NSW Environment Trust (RM08603), as well as the Australian Research Council as part of DP120100338 and FT110100576. This work was supported by an award under the Merit Allocation Scheme on the NCI National Facility at the ANU.

Appendix A. Supplementary material

Supplementary data associated with this article can be found, in the online version, at http://dx.doi.org/10.1016/j.jhydrol.2015.06.067.

References

Alexander, L. et al., 2006. Global observed changes in daily climate extremes of temperature and precipitation. J. Geophys. Res.: Atmos. (1984–2012) 111 (D5).
Allan, R.P., Soden, B.J., 2008. Atmospheric warming and the amplification of precipitation extremes. Science 321 (5895), 1481–1484.
Argüeso, D. et al., 2011. Evaluation of WRF parameterizations for climate studies over Southern Spain using a multistep regionalization. J. Clim. 24 (21), 5633–5651.
Argüeso, D., Hidalgo-Muñoz, J.M., Gámiz-Fortis, S.R., Esteban-Parra, M.J., Castro-Díez, Y., 2012. Evaluation of WRF mean and extreme precipitation over Spain: present climate (1970–99). J. Clim. 25 (14), 4883–4897.
Argüeso, D., Evans, J.P., Fita, L., 2013a. Precipitation bias correction of very high resolution regional climate models. Hydrol. Earth Syst. Sci. Discuss. 10 (6), 8145–8165.
Argüeso, D., Evans, J.P., Fita, L., Bormann, K., 2013b. Temperature response to future urbanization and climate change. Clim. Dyn., 1–17
Argüeso, D., Evans, J.P., Pitman, A.J., Di Luca, A., 2015. Effects of city expansion on heat stress under climate change conditions. PLoS ONE 10 (2), e0117066.
Bacchi, B., Ranzi, R., 1996. On the derivation of the areal reduction factor of storms. Atmos. Res. 42 (1–4), 123–135.
Bengtsson, L., Niemczynowicz, J., 1986. Areal reduction factors from rain movement. Nord. Hydrol. 17 (2), 65–82.
Efron, B., Tibshirani, R.J., 1994. An Introduction to the Bootstrap. CRC Press.
Evans, J.P., McCabe, M.F., 2010. Evaluating a regional climate model's ability to simulate the climate of the South-east coast of Australia. In: IOP Conference Series: Earth and Environmental Science. IOP Publishing, p. 012004.
Evans, J.P., McCabe, M.F., 2013. Effect of model resolution on a regional climate model simulation over southeast Australia. Clim. Res. 56 (2), 131–145.
Evans, J.P., Westra, S., 2012. Investigating the mechanisms of diurnal rainfall variability using a regional climate model. J. Clim. 25 (20), 7232–7247.
Evans, J.P., Argüeso, D., Fita, L., Bormann, K., 2012. NARCliM-Sydney Progress: Evaluation of Simulations. Climate Change Research Centre, University of New South Wales.
Green, J., Xuereb, K., Johnson, F., Moore, G., The, C., 2012. The revised intensity–frequency–duration (IFD) design rainfall estimates for australia – an overview. In: 34th Hydrology and Water Resources Symposium 2012. Engineers Australia, Sydney, pp. 808–815.
Groisman, P.Y. et al., 2005. Trends in intense precipitation in the climate record. J. Clim. 18 (9), 1326–1350.
Gudmundsson, L., Bremnes, J.B., Haugen, J.E., Engen-Skaugen, T., 2012. Technical note: downscaling RCM precipitation to the station scale using statistical transformations – a comparison of methods. Hydrol. Earth Syst. Sci. 16 (9), 3383–3390.
Hardwick Jones, R., Westra, S., Sharma, A., 2010. Observed relationships between extreme sub-daily precipitation, surface temperature, and relative humidity. Geophys. Res. Lett. 37 (22), L22805.
Hay, L.E., Wilby, R.L., Leavesley, G.H., 2000. A comparison of delta change and downscaled GCM scenarios for three mountainous basins in the United States. J. Am. Water Resour. Assoc. 36 (2), 387–397.
Hosking, J.R.M., Wallis, J.R., 2005. Regional Frequency Analysis: An Approach based on L-moments. Cambridge University Press.
IEAust, 1987. Australian Rainfall & Runoff: A Guide to Flood Estimation. Institution of Engineers, Australia, Barton, ACT.
IPCC, 2000. IPCC Special Report on Emission Scenarios. Cambridge University Press, UK.
Jakob, D., 2013. Nonstationarity in extremes and engineering design. In: AghaKouchak, A., Easterling, D., Hsu, K., Schubert, S., Sorooshian, S. (Eds.), Extremes in a Changing Climate. Water Science and Technology Library. Springer, Netherlands, pp. 363–417.
Johnson, F., Sharma, A., 2009. Measurement of GCM skill in predicting variables relevant for hydroclimatological assessments. J. Clim. 22 (16), 4373–4382.
Johnson, F., Sharma, A., 2011. Accounting for interannual variability: a comparison of options for water resources climate change impact assessments. Water Resour. Res. 47 (4), W04508.
Johnson, F., Haddad, K., Rahman, A., Green, J., 2012. Application of Bayesian GLSR to estimate sub daily rainfall parameters for the IFD Revision Project. In: Hydrology and Water Resources Symposium.
Jordan, P., Weinmann, E., Hill, P., Wiesenfeld, C., 2013. Australian Rainfall & Runoff Revision Project: Project 2-Collation and Review of Areal Reduction Factors from Applications of the CRC-FORGE Method in Australia. P2/S2/012, Sinclair Knight Merz.
Kanemaru, K., Masunaga, H., 2012. A satellite study of the relationship between sea surface temperature and column water vapor over tropical and subtropical oceans. J. Clim. 26 (12), 4204–4218.
Lee, T.-C., Chan, K.-Y., Chan, H.-S., Kok, M.-H., 2011. Projections of extreme rainfall in Hong Kong in the 21st century. Acta Meteorol. Sinica 25 (6), 691–709.
Lenderink, G., van Meijgaard, E., 2008. Increase in hourly precipitation extremes beyond expectations from temperature changes. Nat. Geosci. 1 (8), 511–514.
Liew, S.C., Raghavan, S.V., Liong, S.Y., 2013. How to construct future IDF curves, under changing climate, for sites with scarce rainfall records? Hydrol. Process., n/a–n/a
Madsen, H., Rasmussen, P.F., Rosbjerg, D., 1997. Comparison of annual maximum series and partial duration series methods for modeling extreme hydrologic events: 1. At-site modeling. Water Resour. Res. 33 (4), 747–757.
Madsen, H., Arnbjerg-Nielsen, K., Mikkelsen, P.S., 2009. Update of regional intensity–duration–frequency curves in Denmark: tendency towards increased storm intensities. Atmos. Res. 92 (3), 343–349.
Maurer, E.P., Das, T., Cayan, D.R., 2013. Errors in climate model daily precipitation and temperature output: time invariance and implications for bias correction. Hydrol. Earth Syst. Sci. 17 (6), 2147–2159.
Milly, P.C.D. et al., 2008. Stationarity is dead: whither water management? Science 319, 573–573.

Myers, V.A., Zehr, R.M., 1980. A Methodology for Point-to-Area Rainfall Frequency Ratios. US Department of Commerce, National Oceanic and Atmospheric Administration, National Weather Service.
NERC, 1975. Flood Studies Report, vol. II. Natural Environment Research Council, UK.
O'Gorman, P.A., Schneider, T., 2009. The physical basis for increases in precipitation extremes in simulations of 21st-century climate change. Proc. Natl. Acad. Sci. 106 (35), 14773–14777.
Omolayo, A., 1993. On the transposition of areal reduction factors for rainfall frequency estimation. J. Hydrol. 145 (1), 191–205.
Panthou, G., Mailhot, A., Laurence, E., Talbot, G., 2014. Relationship between surface temperature and extreme rainfalls: a multi-time-scale and event-based analysis. J. Hydrometeorol. 15 (5), 1999–2011.
Prodanovic, P., Simonovic, S.P., 2007. Development of Rainfall Intensity Duration Frequency Curves for the City of London under the Changing Climate. Department of Civil and Environmental Engineering, The University of Western Ontario.
Radermacher, C., Tomassini, L., 2012. Thermodynamic causes for future trends in heavy precipitation over Europe based on an ensemble of regional climate model simulations. J. Clim. 25 (21), 7669–7689.
Räisänen, J. et al., 2004. European climate in the late twenty-first century: regional simulations with two driving global models and two forcing scenarios. Clim. Dyn. 22 (1), 13–31.
Rodriguez-Iturbe, I., Mejía, J.M., 1974. On the transformation of point rainfall to areal rainfall. Water Resour. Res. 10 (4), 729–735.
Shaw, S.B., Royem, A.A., Riha, S.J., 2011. The relationship between extreme hourly precipitation and surface temperature in different hydroclimatic regions of the United States. J. Hydrometeorol. 12 (2), 319–325.
Siriwardena, L., Weinmann, P.E., 1996. Derivation of Areal Reduction Factors for Design Rainfalls in Victoria: for Rainfall Durations 18–120 hours.pdf. Cooperative Research Centre for Catchment Hydrology.
Speer, M.S., Wiles, P., Pepler, A., 2009. Low pressure systems off the New South Wales coast and associated hazardous weather: establishment of a database. Aust. Meteorol. Oceanogr. J. 58 (1), 29.
Tebaldi, C., Hayhoe, K., Arblaster, J.M., Meehl, G.A., 2006. Going to the extremes. Clim. Change 79 (3–4), 185–211.
Veneziano, D., Langousis, A., 2005. The areal reduction factor: a multifractal analysis. Water Resour. Res. 41 (7), W07008.
Wasko, C., Sharma, A., 2014. Quantile regression for investigating scaling of extreme precipitation with temperature. Water Resour. Res. 50 (4), 3608–3614.
Wasko, C., Sharma, A., 2015. Steeper temporal distribution of rain intensity at higher temperatures within Australian storms. Nat. Geosci., advance online publication
Westra, S., Alexander, L.V., Zwiers, F.W., 2012. Global increasing trends in annual maximum daily precipitation. J. Clim. 26 (11), 3904–3918.
Woldemeskel, F.M., Sharma, A., Sivakumar, B., Mehrotra, R., 2012. An error estimation method for precipitation and temperature projections for future climates. J. Geophys. Res.: Atmos. 117 (D22), D22104.
Wong, G. et al., 2014. Stochastic model output statistics for bias correcting and downscaling precipitation including extremes. J. Clim. 27 (18), 6940–6959.
Zehr, R.M., Myers, V.A., 1984. Depth-Area Ratios in the Semi-Arid Southwest United States, 40. US Dept. of Commerce, National Oceanic and Atmospheric Administration, National Weather Service.
Zhu, J., Forsee, W., Schumer, R., Gautam, M., 2013. Future projections and uncertainty assessment of extreme rainfall intensity in the United States from an ensemble of climate models. Clim. Change 118 (2), 469–485.